J Therm Anal Calorim (2012) 109:545–553
DOI 10.1007/s10973-012-2216-7

Thermophysical theory of DSC melting peak

V. A. Drebushchak

Bretsznajder Special Chapter

Abstract Melting peak for metals is described with expressions derived from thermophysical consideration of DSC operation. Three parameters govern the shape of the peak: thermophysical coefficient derived from the DSC design, enthalpy of fusion of a sample, and heating rate. Rigorous evaluation yields rather complex expressions, but simplified expressions can be used in common practice. The peak shape is described by two different expressions for two separate stages in the process of metal melting (1) the melting itself and (2) heat relaxation after the melting completion. The validity of the expressions was demonstrated after the experiments on gallium melting. The thermophysical coefficient is shown be affected to small variations by the changes in sample preparation or experimental conditions (melting Ga, In, Zn).

Keywords DSC · Enthalpy of fusion · Heat conduction · Heating rate · Melting peak · Temperature relaxation

Introduction

Melting of metals is used widely in DSC calibration. Onset point is used for the temperature calibration and the area of the peak for the calibration of a heat sensor. It is surprising thing that there are no equations describing the shape of the melting peak so far. When discussing the DSC experiments on melting, several ways are used.

The simplest way is to draw the peak empirically. Four variants of the shape are shown in Fig. 1, three were borrowed from the standards on DSC experiments [1–3] and one from the monograph [4]. The peaks are asymmetric in Fig. 1a, b. DSC signal increases as a straight line from its start up to a maximum and then decreases exponentially. These two shapes differ in the position of the maximum, close to the start or to the end of the peak. Peaks in Fig. 1c, d are completely symmetric, with curving sides in Fig. 1c and straight lines in Fig. 1d. These peaks are used in the references for the discussion of various topics, but the shape of the peak itself is not discussed.

Mathematical approach to the description of the shape of the melting peak is used for the approximation of experimental data. Ref. [5] is the example of such an approach. Numerical fitting of the signal was carried out «with tools borrowed from spectroscopy and chromatography». Two types of functions were used: (1) 'Spectral' (symmetrical) functions "Gaussian," "Lorentzian," and "Voigt"; (2) "Chromatographic" (asymmetrical) functions "exponentially modified Gaussian," "Haarhoff–Van der Linde," and "Pearson IV." Each function has three to five parameters that allow one to improve the approximation. The parameters have no physical sense. This is the main disadvantage of this approach. The parameters of the mathematical function have no relation with the particular properties both of a sample and DSC and can be calculated only after the fitting. No prediction on the shape of the DSC peak is possible.

Most popular approach is the electric modeling of DSC operation. This is a traditional way to analyze thermoanalytical measurements for several decades [6]. The modeling is described in detail in many reports and monographs (see, for example, most fresh monograph by Höhne et al. [4]).

V. A. Drebushchak
Novosibirsk State University, Ul. Pirogova 2, Novosibirsk, Russia 630090

V. A. Drebushchak (✉)
Institute of Geology and Mineralogy SB RAS, Pr. Ac. Koptyuga 3, Novosibirsk, Russia 630090
e-mail: dva@igm.nsc.ru; dva@xray.nsu.ru

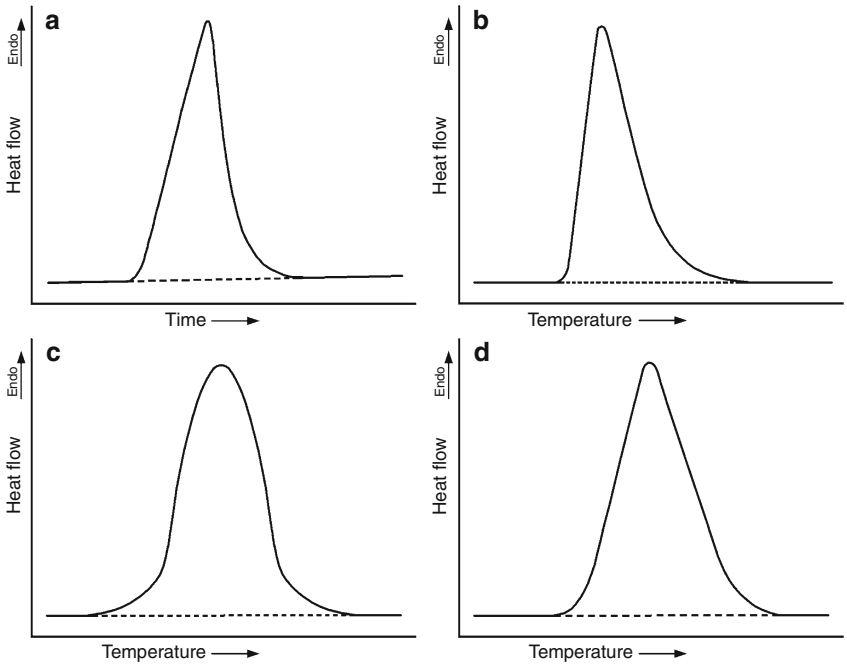

Fig. 1 Empirical shape of the melting peak as detected by DSC from different references: **a** [1], **b** [2], **c** [3], **d** [4]

According to this approach, DSC cell is substituted with an electric circuit containing resistances and capacitors, and the heat flows are substituted with electric currents. DSC signal is considered to be equivalent to the voltage derived from the equations describing the electric current in the analog circuit. The equation itself can be (and usually is) rather complex to contain many parameters in order to describe the signal as accurate as possible. For conventional scheme of DSC cell, the mathematical expression is a differential equation of the second order

$$\begin{aligned}\Phi_{\mathrm{r}}(t) = &-\left(\frac{1}{R}+\frac{2}{R_{\mathrm{MM}}}\right)\Delta T \\ &-\left[C+C_{\mathrm{S}}\left(1+R_{\mathrm{MS}}\left(\frac{1}{R}+\frac{2}{R_{\mathrm{MM}}}\right)\right)\right]\frac{\mathrm{d}\Delta T}{\mathrm{d}t} \\ &-R_{\mathrm{MS}}\cdot C\cdot C_{\mathrm{S}}\frac{\mathrm{d}^2\Delta T}{\mathrm{d}t^2}+(C_{\mathrm{R}}-C_{\mathrm{S}})\frac{\mathrm{d}T_{\mathrm{R}}}{\mathrm{d}t} \\ &+C_{\mathrm{S}}\cdot C_{\mathrm{R}}(R_{\mathrm{MS}}-R_{\mathrm{MR}})\frac{\mathrm{d}^2T_{\mathrm{R}}}{\mathrm{d}t^2},\end{aligned}$$

where ΔT is the signal on the differential thermocouple, and the rest parameters describe the particular elements of the electric circuit (see [4]). Calculated peaks of the melting look very similar to those measured in the experiments. The calculations confirm that the peaks depend on heating rate, heat of fusion, and thermal conductance of the sample. The quantitative relationship among these parameters remains unknown.

Much more rare (and recent) is the thermophysical approach, when the DSC operation is considered directly through the heat flow, enthalpy of fusion, heating rate, etc., without analogy with electric circuits. Equations enabling us to calculate the peak height and width after heating rate, sample mass, enthalpy of fusion, and heat conductivity of the sample holder were published for the first time in Russian textbook [7] (can be downloaded from http://htt.nsu.ru/files/Thermal%20analysis.pdf) and 3 years after in the user magazine in English [8] (can be downloaded from www.mt.com/ta-usercoms). The equations in [7] and [8] are approximate because they were derived after simplified considerations.

The subject of this study is to derive the explicit formulae that will allow us to describe the shape of the melting peak as measured with a DSC. The equations will be derived in the same way as it was performed recently for the calibration coefficient of DSC as a function of temperature [9]. The latter did allow us do develop optimal calibration procedure [10] that is used in practice today [11–14].

Theory

Melting

Figure 2 shows DSC cell with two crucibles at their positions, empty (reference, R) and with a sample (S). A heat portion of

$$\mathrm{d}Q_{\mathrm{R}} = c_{\mathrm{C}}m_{\mathrm{C}}\mathrm{d}T, \quad (1)$$

is necessary to increase the temperature of crucible R by $\mathrm{d}T$, where c_{C} is the specific heat of the material that the crucible is made of, and m_{C} is its mass. Crucible S is

identical to R in ideal differential scheme of DSC. The heat necessary to increase its temperature by dT is

$$dQ_S = (c_C m_C + c_S m_S)dT, \quad (2)$$

where c_S m_S is the heat capacity of the sample. If heating DSC cell with a constant heating rate $\beta = dT/dt$, heat flows ($W = dQ/dt$) to crucibles R and S differ from one another:

$$W_R = c_C m_C \beta, \quad (3)$$

$$W_S = (c_C m_C + c_S m_S)\beta, \quad (4)$$

$$W_S - W_R = c_S m_S \beta = W_0. \quad (5)$$

W_0 is known as a baseline. The difference in the heat fluxes between crucibles R and S is due to the difference in their temperatures

$$\Delta W = -\left(\frac{S_1\lambda}{l} + 4S_2\varepsilon\sigma T^3\right)(T_S - T_R), \quad (6)$$

where S_1 is the area of a contact between crucible and sensor, λ is the coefficient of heat conductivity, l is the distance between a heat source and a sample holder, S_2 is the area of a crucible exposed to the radiation, ε is the emissivity of the substance which the crucible is made of, and σ is the Stefan's constant [9]. The first term in the brackets is for the heat conduction and the second one is for the radiation. In combining Eqs. 5 and 6, we receive

$$c_S m_S \beta = -\left(\frac{S_1\lambda}{l} + 4S_2\varepsilon\sigma T^3\right)(T_S - T_R). \quad (7)$$

This is the key formula for the DSC calibration coefficient as a function of temperature [9]. The function can be derived after consideration of differential thermocouple and the Seebeck coefficient. Here, we will use it to analyze thermal flows and processes during the metal melting. We emphasize the case of a metal because will not discuss the temperature gradient, considering the same temperature throughout the crucible. The duration of the melting is also considered too short to simplify Eq. 7 with

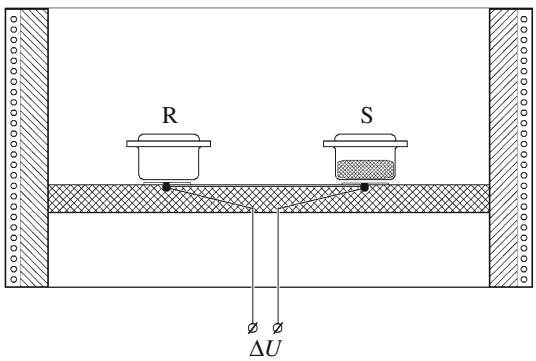

Fig. 2 DSC cell with empty reference (R) crucible and that filled with a sample (S)

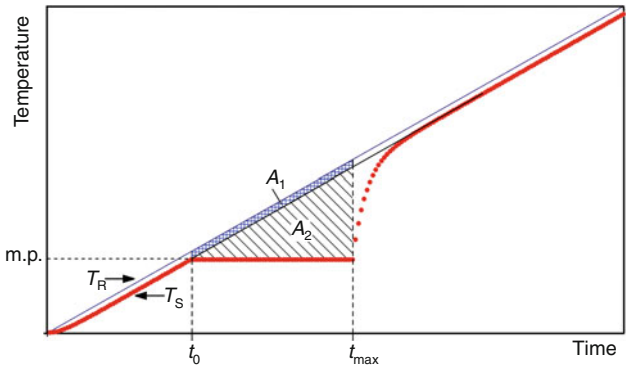

Fig. 3 Temperature against time for reference and sample crucibles during the experiment on metal melting. Melting point is reached at t_0. The whole sample becomes liquid at t_{max}. See explanations for areas A_1 and A_2 in the text

$$K = \left(\frac{S_1\lambda}{l} + 4S_2\varepsilon\sigma T^3\right) \approx \text{const}. \quad (8)$$

Temperature of crucibles R and S during the experiment on metal melting is shown in Fig. 3. The difference in temperature is

$$T_S = T_R - \frac{c_S m_S \beta}{K} = T_R - \Delta T. \quad (9)$$

Thermophysical analysis of DSC operation with Eqs. 1–9 is described in many reports and monographs, including those with electric circuit analogy. The only difference between previous works and current one is in the coefficient K. It was considered a function of thermal conductivity (S_1, λ, l) elsewhere, but we add the heat radiation. This point was the last in thermophysical consideration. After Eq. 9, only electric analogy was considered. Here, we will continue analysis of thermal processes.

Sample starts to melt at time t_0 and its temperature remains constant up to the complete melting at t_{max}. During this period, the difference in temperature between the crucibles increases linearly $\Delta T + \beta(t - t_0)$ and the heat flow is spent on the melting

$$W = K(\Delta T + \beta(t - t_0)). \quad (10)$$

Let's substitute variables

$$\tau = t - t_0; \quad \tau_{max} = t_{max} - t_0. \quad (11)$$

The total heat spent on the melting is calculated according to

$$\int_0^{\tau_{max}} W d\tau = K \int_0^{\tau_{max}} (\Delta T + \beta\tau) d\tau. \quad (12)$$

On the left-hand side, the integration yields the total enthalpy of fusion:

$$\int_0^{\tau_{max}} W d\tau = qm_S, \tag{13}$$

where q is the specific enthalpy of fusion. On the right-hand side, we have two contributions

$$K\int_0^{\tau_{max}} (\Delta T + \beta\tau)d\tau = K\Delta T\tau_{max} + \frac{K\beta}{2}\tau_{max}^2. \tag{14}$$

In using Eq. 9, we have

$$K\Delta T\tau_{max} = c_S m_S \beta \tau_{max}. \tag{15}$$

Thus, after the integration, Eq. 12 transforms into

$$\frac{K\beta}{2}\tau_{max}^2 + c_S m_S \beta \tau_{max} - qm_S = 0, \tag{16}$$

which allows us to calculate the duration of the melting τ_{max}:

$$\begin{aligned}\tau_{max} &= \frac{-c_S m_S \beta + \sqrt{c_S^2 m_S^2 \beta^2 + 2K\beta q m_S}}{K\beta} \\ &= -\frac{c_S m_S}{K} + \sqrt{\left(\frac{c_S m_S}{K}\right)^2 + \frac{2qm_S}{K\beta}}\end{aligned} \tag{17}$$

Equation 17 contains only two different terms, but it is not quite easy to analyze it. We can simplify it if one of two terms is much greater than the other. The two terms in Eq. 17 are there because the total heat spent on the melting is a sum of two contributions (see Eq. 14). Each contribution is shown in Fig. 3 as the crosshatched area, A_1 proportional to time and A_2 proportional to the square of time. Usually

$$\frac{A_1}{A_1 + A_2} \ll 1 \tag{18}$$

Omitting term A_1, we receive simplified expression from (17):

$$\tau_{max} = \sqrt{\frac{2qm_S}{K\beta}}. \tag{19}$$

According to Eq. 10, DSC signal increases during the melting from baseline W_0 up to the maximum W_{max} and the increase is

$$W_{max} - W_0 = K\beta\tau_{max} = \sqrt{2Kqm_S\beta}. \tag{20}$$

The greatest difference in temperature (peak hight) is

$$T_{max} - T_{onset} = \beta\tau_{max} = \sqrt{\frac{2qm_S\beta}{K}}. \tag{21}$$

Equations 19–21 were derived in [7] and [8] after simplified considerations and here these are the simplified expression after rigorous considerations. The parameters of the melting peak are shown in Fig. 4 for temperature difference between crucibles R and S against time.

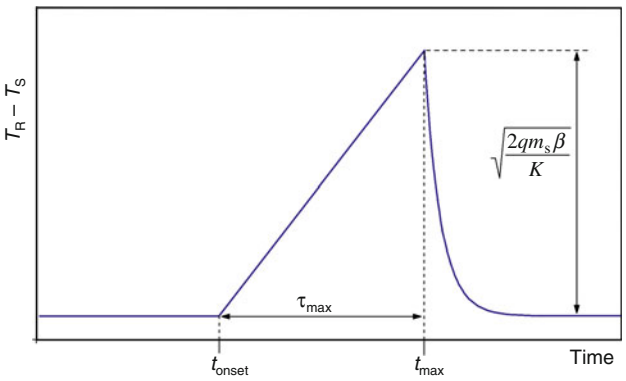

Fig. 4 Temperature difference $T_R - T_S$ measured with differential thermocouple as presenting the results of the experiment on metal melting. The melting peak parameters are shown

Temperature relaxation

After completion of the melting, crucible S contains the melt at the melting point T_{onset} but the temperature of crucible R is $T_{onset} + \beta\tau_{max}$ (the increase in temperature for the time of melting) + $c_S m_S \beta/K$ (=ΔT, see Eq. 9, the difference at the start of the melting). For the sake of simplicity, let the heat capacity of solid sample be equal to that of liquid sample. Now we will consider the relaxation of temperature difference between the cold melt and hot surroundings. The moment of melting completion is the new starting point for the relaxation. Difference in temperature between the crucibles will change in time. Excess heat flow to crucible S is

$$W(t) = K(T_R(t) - T_S(t)) \tag{22}$$

or

$$dQ = K(T_R(t) - T_S(t))dt. \tag{23}$$

The increment in temperature is

$$d(T_R(t) - T_S(t)) = dT_R(t) - dT_S(t)) \tag{24}$$

$$dT_R(t) = \beta dt \tag{25}$$

$$dT_S(t) = \frac{dQ}{c_C m_C + c_S m_S}. \tag{26}$$

T_R increases according to Eq. 25 because DSC cell is heated with constant heating rate β. T_S increases according to Eq. 26 because of heat flow (23). Substituting Eqs. 23, 25, and 26 for right-hand side of Eq. 24, we have

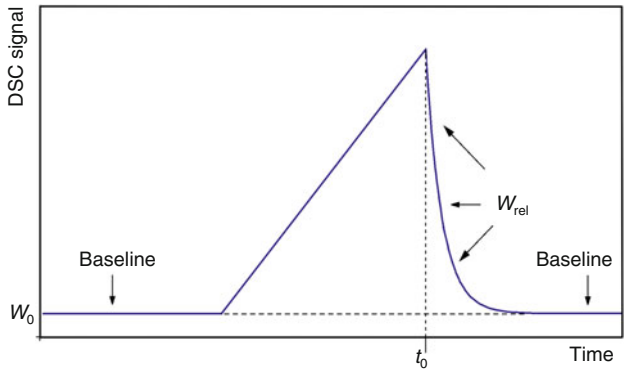

Fig. 5 Relaxation of temperature difference between the melt and surroundings in DSC cell. W_0 is the baseline and W_{rel} is the excess heat spent for the relaxation

$$\mathrm{d}(T_R - T_S) = (c_S m_S \beta - K(T_R - T_S)) \frac{\mathrm{d}t}{c_C m_C + c_S m_S}, \tag{27}$$

$$\mathrm{d}(T_R - T_S) = -\left((T_R - T_S) - \frac{c_S m_S \beta}{K}\right) \frac{K\mathrm{d}t}{c_C m_C + c_S m_S}, \tag{28}$$

$$\mathrm{d}\ln\left(T_R - T_S - \frac{c_S m_S \beta}{K}\right) = -\frac{K\mathrm{d}t}{c_C m_C + c_S m_S}. \tag{29}$$

The solution for this differential equation is

$$T_R - T_S = \frac{c_S m_S \beta}{K} + \mathrm{A}\exp\left(-\frac{Kt}{c_C m_C + c_S m_S}\right). \tag{30}$$

Constant A is calculated after the limits of integration and finally we have

$$\begin{aligned} W &= K(T_R - T_S) \\ &= c_S m_S \beta + \sqrt{2Kqm_S\beta}\,\exp\left(-\frac{Kt}{c_C m_C + c_S m_S}\right) \\ &= W_0 + W_{rel}. \end{aligned} \tag{31}$$

Figure 5 shows DSC signal consisting of two contributions, constant W_0 (baseline) and variable W_{rel} (decreasing with time). It is the latter that describes the temperature relaxation after the melting.

Testing the equations

Testing the validity of the derived equations

Equations 19–21 are related with simple transformations. To demonstrate the validity of all these equations, it is enough to test the linear relationship between the peak height (in temperature or in watts) and square root of the product of sample mass by heating rate. Such a test was performed for the first time in [15]. Four samples of different mass (0.053, 0.846, 3.425, and 6.301 mg) were measured at heating rates between 1 and 20 K min^{-1}. Unfortunately, the detailed information about the experiments was not reported, only the figure. Experimental points were found to fit very well to a straight line. Surprisingly, the range of experimental values $\sqrt{m\beta}$ plotted turned out to be very small, less than 1.5 (mg K s^{-1})$^{1/2}$. It seems very strange because even the sample of 0.846 mg (second to the smallest sample) at the heating rate of 20 K min^{-1} yields 4.1 (mg K s^{-1})$^{1/2}$. It looks like the test was especially limited in the product of mass by heating rate in order not to show the high values.

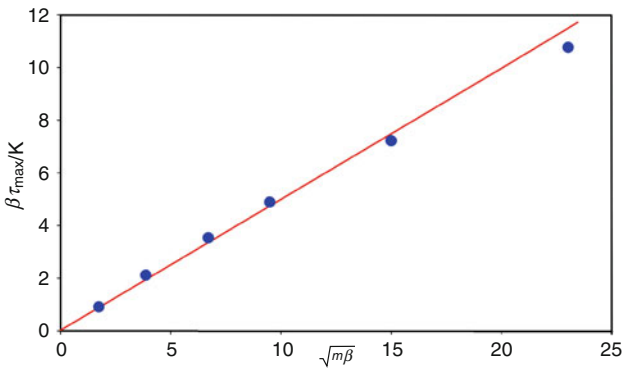

Fig. 6 Experimental values $\beta\tau_{max}$ against calculated $\sqrt{m\beta}$ (*filled circles*). Ideal agreement between simplified equations and experiment is to be a *straight line*. The deflection downwards of the points with high values proves the validity of the model and simplification of Eq. 17

Table 1 Experimental conditions (sample mass and heating rate) and the results (melting duration) of Ga melting

Run	m/mg	β/K min^{-1}	$\sqrt{m\beta}$	$\beta\tau_{max}$/K
1	3.04	1	1.74	0.91
2	15.00	1	3.87	2.11
3	15.00	3	6.71	3.53
4	15.00	6	9.49	4.89
5	15.00	15	15.00	7.21
6	35.41	15	23.05	10.77

Here, we will test the equations for high values. Experimental testing of Eqs. 19–21 was performed with DSC-204 Netzsch in standard Al crucibles. Experimental data on the gallium melting for the test are listed in Table 1. The variables are range in wide limits, more than ten times each: β from 1 to 15 K min^{-1} and m from 3 to 35 mg. The square root ranges also more than ten times, from 1.74 to 23.05. The test itself is in Fig. 6, $\sqrt{m\beta}$ versus $\beta\tau_{max}$. Experimental points fall on the straight line, supporting the validity of the equations derived.

The best linear behavior is for small values, with the deflection downwards for high values. Let us remember that Eqs. 19–21 were derived on the assumption that the

enthalpy of fusion is much greater than the product of heat capacity by heating rate, $\beta\tau_{max}$ (Eq. 18). The longer is the melting (τ_{max}), the greater is the heat capacity contribution. This contribution decreases experimental value $\beta\tau_{max}$ as compared with simplified formula $\sqrt{m\beta}$. Thus, the deflection downwards of experimental points in Fig. 6 for high values of $\sqrt{m\beta}$ does support our thermophysical model. We may suppose that the deflection downwards is the reason why Schawe [15] has limited the greatest value of his experimental points with 1.5 (mg K $s^{-1})^{1/2}$. The experimental points with larger values do not support simplified considerations yielding Eqs. 19–21 [7, 8].

Melting point of gallium (atomic weight 69.723) is 302.9146 K (29.7646 °C) [16] and its enthalpy of fusion is 80.097 ± 0.032 J g^{-1} [17]. Heat capacity of Ga near the melting point is about 26 J mol^{-1} K^{-1} or 0.37 J g^{-1} K^{-1}, nearly the same in crystal and liquid states [18]. The last point makes Ga very suitable for our purpose, because the heat capacity is the same for crystalline and liquid metal in our model (see the first paragraph in "Temperature relaxation" section).

For the experimental point with the longest melting (35.41 mg and 15 K min^{-1}) the enthalpy increment due to the baseline is about 5% (0.37•10.77 ≈ 4 J g^{-1}) of the enthalpy of fusion. Thus, the last experimental points in Fig. 6 deflect downwards because the large enthalpy increment due to the heat capacity makes the simplification of Eq. 17 into 19 incorrect.

Thermophysical coefficient K

User cannot change technical features of a DSC, but it would be useful for him to know the value of thermophysical coefficient K affecting the melting peak. The value can be derived from the same experimental data listed in Table 1. We can derive from Eq. 21

$$K = \frac{2qm_S\beta}{(\beta\tau_{max})^2}. \tag{32}$$

All the values in the equations except q are listed in Table 1. For example, for the sample of 15 × 10^{-3} g at the heating rate of 0.1 K s^{-1} the value of $\beta\tau_{max}$ is 4.89 K. The thermophysical coefficient

$$K = \frac{2 \cdot 80.097 \cdot 0.015 \cdot 0.1}{(4.89)^2} = 0.01005 \text{ W K}^{-1} = 10 \text{ mW K}^{-1}. \tag{33}$$

This value is valid only for 300 K because thermophysical properties of materials, which DSC made of, depend on temperature (thermal conductivity, heat capacity, etc.). As the K also depends on the heat radiation, its value increases with temperature (see Eq. 7).

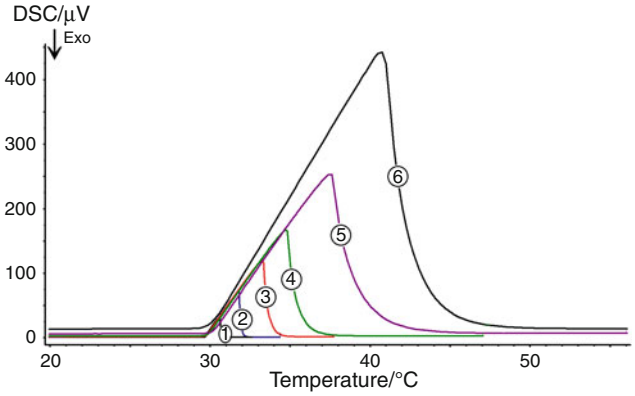

Fig. 7 Uniform shape of melting peak for runs 1–5 is violated for run 6. Slight variation in thermophysical coefficient K is due to the variation in sample preparation (see text)

Coefficient K governs the calibration coefficient of DSC $k(T)$. The latter is

$$k(T) = \frac{\varepsilon(T)}{S_1\lambda/l + 4S_2\varepsilon\sigma T^3}, \tag{34}$$

where $\varepsilon(T)$ is the Seebeck coefficient of the thermocouple used as the heat flow sensor [9]. In comparing (34) with (8), we see that

$$K\,k(T) = \varepsilon(T). \tag{35}$$

Thermophysical coefficient K cannot be changed in experiments at will like the sample mass or heating rate. But, significant variations in the value of coefficient K can be observed sometimes. First case is shown in Fig. 7. Five of six runs (1–5) on Ga melting have nearly the same line of increasing signal from the onset point to the maximum of the melting peak. The last run differs significantly. The line increases surely steeper than the rest ones. The reason is in the sample preparation. For runs 1–5, solid metal sample was put onto the bottom of cold crucible (room temperature), then cooled and heated to the melting. In the last run, solid metal sample was put into the hot crucible (40–50 °C) and pressed to the bottom in order to melt it before cooling. Then the crucible with liquid Ga was cooled down to the sample freezing, and then the run was performed like the others. The manipulations with the sample in the sixth run allowed the sample to contact better with the crucible, increasing the heat conduction between the sample and crucible. This makes a variation in the K value, increasing heat flow and DSC signal, but decreasing the duration of melting τ_{max}.

Another example of the variations in thermophysical coefficient K can be seen in Fig. 8. This is the melting of zinc. All the runs are with the same sample. Crucible was placed inside DSC cell and measured 21 times according to the same temperature program, one by one. It is evident

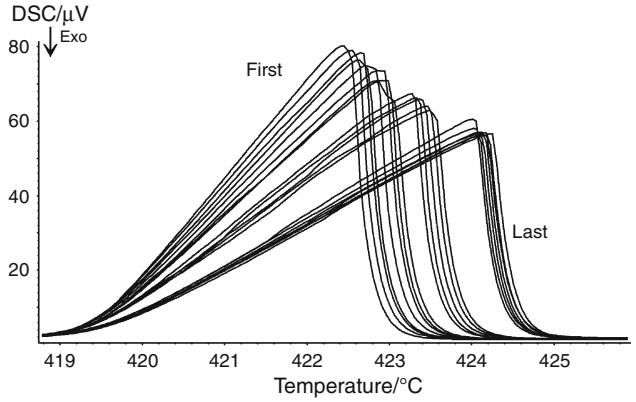

Fig. 8 Melting of the same sample of Zn (21 runs). Slope of the peak decreases with time due to the change in thermophysical coefficient K (oxidation of sample surface)

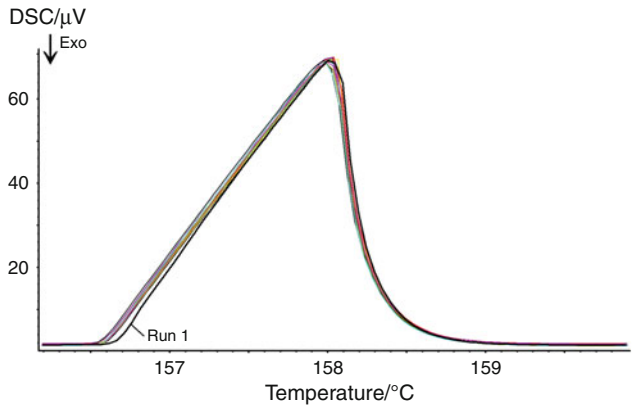

Fig. 9 Melting of the same sample of In (13 runs). Slope of the peak remains unchanged. Only the first run differs from the rest

from the figure that the slope of the straight line of the melting peak decreases with time (with the number of a run). The reason is in the oxidation of the sample. After the completion of the experiments, the sample was found to change its color from metal luster to iridescent play of black colors. Zinc oxide on the surface of a sample is a bad heat conductor, decreasing heat exchange and DSC signal, but increasing the duration of melting τ_{max}. In contrast, indium is not oxidized during the melting–freezing runs and similar experiments with indium do not reveal the changes in the slope of the melting peak (Fig. 9). Thermophysical coefficient K remains constant in experiments with indium.

Logarithmic heating of cold liquid after melting

In contrast to the melting of metal described with Eqs. 19–21, the logarithmic relaxation of the peak was known for a long time. Electric analog models have yielded similar function of time:

$$\Delta T = k_1 \exp\left(\frac{-t}{\tau}\right) + k_2, \tag{36}$$

with $\tau = C_S{\cdot}R$, where C_S is the heat capacity of the sample and R is the thermal resistance, which "must be determined by calibration" [4]. Our Eq. 31 is very similar, but with explicit expressions for coefficients k_1, k_2, and τ:

$$W = c_S m_S \beta + \sqrt{2Kqm_S\beta}\exp\left(-\frac{Kt}{c_C m_C + c_S m_S}\right) = W_0 + W_{rel}.$$

So, it is not necessary to test the validity of the temperature function, but rather the values of the coefficients as predicted by theory. To test the equations against the experimental data, we have to transform a DSC signal

$$\ln(W - W_0) = a - bt, \tag{37}$$

where

$$a = \frac{1}{2}\ln(2Kqm_S\beta) \quad \text{and} \quad b = \frac{K}{c_C m_C + c_S m_S} \tag{38}$$

and then to calculate the coefficients a and b by the least squares. The results of these calculations for runs 1, 2, and 4 are shown in Fig. 10. Very straight lines prove the validity of logarithmic function once again. The coefficients (with excess digits) are shown in Table 2. For every run, the calculations were carried out for 25 points from $t = 6$ s to $t = 30$ s with the step of 1 s. The starting point ($t = 0$) is assigned to the first value decreasing after the

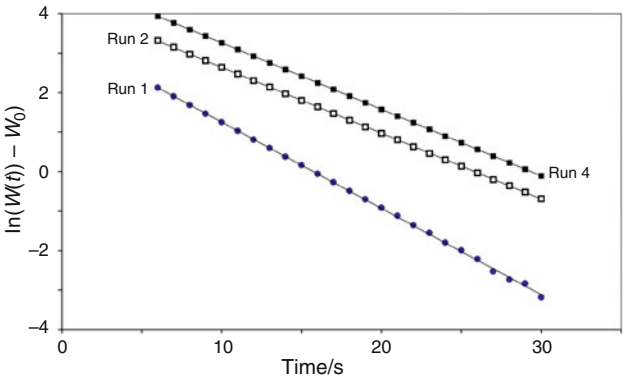

Fig. 10 Kinetics of temperature relaxation after Ga melting completion for runs 1 (*filled circles*), 2 (*empty squares*), and 4 (*filled squares*)

Table 2 Coefficients a and b for thermal relaxation after the melting peak as calculated according to Eq. 37 with least squares

Run (i)	a_i	b_i
1	3.4382	0.2186
2	4.3083	0.1669
4	4.9446	0.1686

maximum. Accuracy of the starting point identification (δt) is about 1 s, and, hence, the error in the evaluation of the signal amplitude is $b_i\delta t$. Let's start the test from the a_i coefficients:

Run 1: $a_1 = 3.44 \pm 0.22$.
Run 2: $a_2 = 4.31 \pm 0.17$.
Run 4: $a_4 = 4.94 \pm 0.17$.

Runs 1 and 2 are with the same heating rate but with the sample mass of 3.04 and 15 mg, respectively. The difference between them is to be

$$a_2 - a_1 = \frac{1}{2}\ln\left(\frac{15}{3.04}\right) = 0.80,$$

which is close to the calculated value

$$a_2 - a_1 = 0.87 \pm 0.39.$$

Runs 2 and 4 are with the same sample mass but with the heating rates of 1 and 6 K min^{-1}, respectively. The difference between them is to be

$$a_4 - a_2 = \frac{1}{2}\ln 6 = 0.90,$$

which agrees with the calculated value within the limits of error

$$a_4 - a_2 = 0.63 \pm 0.34.$$

Now let us test the b_i coefficients. They do not depend on the starting point of the set, and the coefficients b_2 and b_4 must be equal to each other because the sample is the same in both runs. This is true: values 0.1669 and 0.1686 derived from the experiment differ by less than 1%. It is very good agreement. According to Eq. 38, coefficients b_1 and b_2 must differ from one another because runs 1 and 2 differ in sample mass m_S:

$$\frac{b_1}{b_2} = \frac{c_C m_C + c_S m_{S2}}{c_C m_C + c_S m_{S1}}. \tag{39}$$

Crucible mass is 38 mg, heat capacity of aluminum is 24.35 J mol^{-1} K^{-1} or 0.90 J g^{-1} K^{-1} [18]. Heat capacity of gallium is 0.37 J g^{-1} K^{-1} (see above). Thus, we have measured

$$\frac{b_1}{b_2} = \frac{0.2186}{0.1669} \approx 1.31$$

and calculated after theory

$$\frac{c_C m_C + c_S m_{S2}}{c_C m_C + c_S m_{S1}} = \frac{0.90 \cdot 0.038 + 0.37 \cdot 0.015}{0.90 \cdot 0.038 + 0.37 \cdot 0.00304} \approx 1.13.$$

The difference between measured and calculated values is large enough, about 15%. Let us compare our "thermophysical" Eq. 31 with "electrical" Eq. 36. The latter predicts that the coefficient b_i depends only on the heat capacity of the sample (on the sample mass in our runs 1 and 2):

$$\frac{b_1}{b_2} = \frac{c_S m_{S2}}{c_S m_{S1}} = \frac{15}{3.04} \approx 4.93. \tag{40}$$

This calculated result differs much greater from the experiment than that after Eq. 39.

Conclusions

DSC peak of metal melting consists of two parts, isothermal heat consumption during the melting and heat relaxation of cold melt. Thermophysical consideration of the heat flows inside a DSC cell has allowed us to derive the Equations describing the shape of the peak. Three parameters govern mainly the melting: sample mass m, heating rate β, and thermophysical coefficient K. The two first parameters can be changed in the experiment at will, but not the last one.

Experimental testing of the derived equations did approve their validity. DSC peaks of Ga melting with different sample mass and different heating rates obey the relationships predicted by the theory, including the downward deflection from a straight line derived recently from the simplified consideration [7, 8]. The greatest discrepancy between thermophysical theory and experiment were found in the relaxation part of the peak, of about 15%. Nevertheless, this discrepancy is much less as compared with the predictions of electric modeling of DSC.

The results of this work can be useful for the planning of DSC experiments. Thermophysical approach is simpler than the electric analogy because the steps of constructing electric circuit and interpreting relations between thermal and electric values are omitted. Students readily realize it when studying thermal analysis and calorimetry at the Novosibirsk State University.

References

1. ASTM E 793 Enthalpies of fusion and crystallization by differential scanning calorimetry.
2. ASTM E 967 Temperature calibration of differential scanning calorimeters and differential thermal analizers.
3. ISO 11357 Plastics—differential scanning calorimetry. Part 3: determination of temperature and enthalpy of melting and crystallization.
4. Höhne GWH, Hemminger WF, Flammersheim H-J. Differential scanning calorimetry. Berlin: Springer; 2003. p. 298.
5. Popa VT, Segal E. Shape analysis of DSC ice melting endotherms: towards an estimation of the instrumental profile. J Therm Anal Calorim. 2002;69:149–61.
6. Drebushchak VA. From electrical analog to thermophysical modeling of DSC. J Therm Anal Calorim. 2011;105:495–500.

7. Drebushchak VA, Shvedenkov GYu. Thermal Analysis Textbook. Novosibirsk: Novosibirsk State University; 2003. p. 114. (in Russian).
8. Schawe J. Evaluation and interpretation of peak temperatures of DSC curves. Part 1: basic principles. Mettler-Toledo UserCom. 2006;23:6–9.
9. Drebushchak VA. Calibration coefficient of a heat-flow DSC—part 1. Relation to the sensitivity of a thermocouple. J Therm Anal Calorim. 2004;76:941–7.
10. Drebushchak VA. Calibration coefficient of a heat-flow DSC—part II. Optimal calibration procedure. J Therm Anal Calorim. 2005;79:213–8.
11. Markin AV, Letyanina IA, Ruchenin VA, Smirnova NN, Gushchin AV, Shashkin DV. Heat capacity and standard thermodynamic functions of triphenylantimony dimethacrylate over the temperature range from (0 to 400) K. J Chem Eng Data. 2011;56:3657–62.
12. Matsko MA, Vanina MP, Echevskaya LG, Zakharov VA. Study of the compositional heterogeneity of ethylene-1-hexene copolymers via thermal fractionation with the use of differential scanning calorimetry. Polym Sci. 2011;53A:296–302.
13. Pet'kov VI, Firsov DV, Markin AV, Sukhanov MV, Smirnova NN. Thermodynamic properties of $NaZr_2(AsO_4)_3$. Inorg Mater. 2011;47:178–82.
14. Letyanina IA, Smirnova NN, Markin AV, Ruchenin VA, Larina VN, Sharutin VV, Molokova OV. Thermodynamics of tetraphenylantimony acetophenoneoxymate. J Therm Anal Calorim. 2011;103:355–63.
15. Schawe J. Evaluation and interpretation of peak temperatures of DSC curves. 2: examples. Mettler-Toledo UserCom. 2006;24:11–5.
16. Preston-Thomas H. The International Temperature Scale of 1990 (ITS-90). Metrologia. 1990;27:3–10.
17. Archer DG. The enthalpy of fusion of gallium. J Chem Eng Data. 2002;47:304–9.
18. Glushko VP et al. (ed) (1981) Thermodynamic properties of individual substances, 4 vols. Nauka, Moscow (in Russian).